



Manganese-Doped Carbon Dots Via Inner Filter Effect for the Sensitive Detection of Tetracycline in Poultry Meat Samples

Ke Su¹, Guoqiang Xiang^{1,2*}, Yunlong Zhang¹, Xin Wang¹, Linhui Wang¹,
Xinrong Jin¹, Bocong Li² and Gao Huang¹

¹School of Chemistry and Chemical Engineering, Henan University of Technology, Zhengzhou, 450001, P. R. China.

²Engineering Technology Research Center for Grain and Oil Food, State Administration of Grain, Henan University of Technology, Zhengzhou, 450001, P.R. China.

Authors' contributions

This work was carried out in collaboration among all authors. Author GX designed the study, managed the literature searches, wrote the protocol, and wrote the first draft of the manuscript. Author GH performed the statistical analysis, Authors KS, YZ, XW and LW prepared the CDs, optimized the analytical procedure, and analyzed the real sample. Author XJ and BL characterized the CDs and managed the supervision. All authors read and approved the final manuscript.

Article Information

DOI: 10.9734/AJOCS/2021/v10i119085

Editor(s):

(1) Dr. SungCheal Moon, Korea Institute of Materials Science (KIMS), Republic of Korea.

Reviewers:

(1) Kenny Ganie, Universiti Teknologi PETRONAS, Malaysia.

(2) Ali Abd AlHassan Kidhim, Al Muthanna University, Iraq.

Complete Peer review History: <https://www.sdiarticle4.com/review-history/70742>

Original Research Article

Received 01 May 2021
Accepted 12 July 2021
Published 13 July 2021

ABSTRACT

In this study, a rapid and sensitive analytical method has been developed to detect tetracycline hydrochloride (TC) using manganese-doped carbon dots (Mn-CDs) prepared by one-step hydrothermal procedure using 1-(2-pyridinylazo)-2-naohtalenol (PAN) and MnCl₂ as precursor reagents. The obtained Mn-CDs showed an ultraviolet emission at 360 nm with an excitation wavelength of 300 nm. TC has a strong characteristic absorption peak at 356 nm, which has a large spectral overlap with the emission band of the Mn-CDs. The fluorescence intensity (FI) of Mn-CDs at 360 nm is linearly quenched within the TC concentration range of 0.1-200 μM. The developed

*Corresponding author: E-mail: xianggq@126.com;

assay for the detection of TC was based on an inner filter effect (IFE) mechanism and is rapid, sensitive, and was successfully applied for the determination of TC in different poultry meat samples with satisfactory results.

Keywords: Carbon dots; tetracycline hydrochloride; inner filter effect; poultry meat.

1. INTRODUCTION

Tetracycline antibiotics (TCs) are low-cost, broad-spectrum antibacterial agents that sterilize at high concentrations and have been widely used in aquaculture and veterinary medicines to promote the rapid growth of animals [1]. Eight types of Tetracycline antibiotics are currently commercially available and of these, oxytetracycline hydrochloride (OTC), tetracycline hydrochloride (TC), chlortetracycline hydrochloride (CTC), and doxycycline hydrochloride (DC) are commonly administered to food-producing animals in China [2]. In recent years, the abundant – and in some cases improper – use of TCs has caused TC residues to appear in animal-based foods, which may be toxic and dangerous for humans [3,4]. Additionally, when consumed for long periods, low doses of TCs in food can lead to drug-resistant bacteria in humans [5]. In China, the maximum residue limits (MRLs) of TCs were set at 0.1, 0.3, and 0.6 mg g⁻¹ in the muscle, liver, and kidneys for all animal species, respectively which are identical to those of EU standards [6]. To ensure confidence and to limit the TCs residues that appear in animal products, accurate detection and quantitative determination of TCs in edible tissues is of paramount importance.

Various methods have been developed to assay TCs, especially traditional techniques, such as high-performance liquid chromatography (HPLC) [7,8], LC with tandem mass spectrometry (LC-MS) [9,10], capillary electrophoresis (CE) [11], chemiluminescence [12], and colorimetric analysis [13,14]. However, these methods all tend to require sophisticated and expensive instrumentation and/or complicated sample preparation processes. Therefore, a simple, economical, sensitive, and selective method for the detection of TCs is desired. Fluorescence-based methods are generally considered to be more desirable methods because of their sensitivity and simplicity. This has led to the development of a series of fluorescent sensors to detect non-fluorescent TCs, such as silver nanoclusters [15], silicon nanoparticles [16], metal-organic coordination polymers [17,18],

Eu³⁺-based nanoparticles [19-21], CdTe quantum dots, CdTe/ZnS quantum dots [22,23], and carbon dots [24-27]. Among these fluorescent probes, most of them need complicated synthesis procedure and they are cytotoxic, mainly due to the introduction of metal ions. However, carbon dots (CDs), as multifunctional fluorescent probe, have been widely concerned by researchers due to their unique advantages, such as easy to prepare, good stability, low cytotoxicity, high fluorescence quantum yield and flexible surface functionalization [28-31]. Therefore, it is of great significance to develop fluorescent probe for TC based on CDs.

Herein, Mn-CDs with high fluorescence quantum yield (QY) were synthesized through one-step hydrothermal procedure using PAN as the carbon source and MnCl₂ as the dopant. The obtained Mn-CDs have an ultraviolet emission band at 360 nm, which has large spectral overlap with the absorption peak (356 nm) of TC, which gives TC a strong IFE on FI the Mn-CDs. The FI of Mn-CDs (360 nm) was quantitatively quenched with the adding of different concentrations of TC. The analytical performance of the assay with IFE mechanism was evaluated in detail and showed that this method could detect TC in poultry meat samples with satisfactory results.

2. EXPERIMENTAL DETAILS

2.1 Apparatus and Reagents

The fluorescence emission spectrum of Mn-CDs was recorded by a F-6000 fluorescence spectrophotometer (Shimadzu), while the fluorescence lifetime of Mn-CDs was measured with a FL-TCSPC fluorescence spectrophotometer (Horiba Jobin Yvon, France). TEM images were captured on a JEM-2011 transmission electron microscope (TEM). The elemental compositions of Mn-CDs were confirmed by a Thermo Escalab 250Xi X-ray photoelectron spectrometer (XPS). Fourier-transform infrared (FT-IR) spectra in KBr were collected on a WQF-510 FT-IR spectrometer (Beijing Rayleigh Analytical Instrument Co., Ltd., Beijing, China). Absorption spectra were

recorded on an ultraviolet-visible (UV-Vis) spectrophotometer (Shimadzu, UV-2450).

PAN, TC, OTC, CTC, DC, trichloroacetic acid (TCA), ethylenediaminetetraacetic acid disodium(EDTA), disodium hydrogen phosphate dehydrate (Na_2HPO_4), ascorbic acid (AA), citric acid (CA), urea, L-lysine (Lys), L-methionine (Met), L-Arginine (Arg), L-histidine (His), L-phenylalanine (Phe), L-tyrosine (Tyr), α -lactose (α -Lac), lactulose (Lac), D-fructose (Fru), sucrose (Sur), glucose (Glu), and D-mannose (Man) were purchased from Aladdin (<http://www.aladdin-e.com>, Shanghai, China). Different kinds of metal salts were obtained from Xiya Reagent (<http://www.xiyashiji.com>, Linyi, China). The pH of testing solutions was controlled by Britton-Robinson (BR) buffer solutions. All chemical reagents were in analytically pure level and used as received without further purification. Deionized water ($18 \text{ M}\Omega \text{ cm}^{-1}$) was used throughout all experiments.

2.2 Synthesis of Mn-CDs

Mn-CDs were synthesized according to a published literature with slightly modification [32]. PAN (0.20 mmol) and $\text{MnCl}_2 \cdot 4\text{H}_2\text{O}$ (0.40 mmol) were mixed with 10 mL of ethanol, and the mixture was stirred for 10 min. The resulting solution was then transferred to a Teflon autoclave (60 mL), which was tightly sealed and then heated in an oven to $180 \text{ }^\circ\text{C}$ for 4 hours. After the reaction, the autoclave was cooled naturally to room temperature, and 20 mL of deionized water was added to the obtained solution. And the insoluble substances in the solution were separated by centrifugation (11,000 rpm) for 30 min. After centrifugation, the Mn-CDs powder was obtained via vacuum freeze-drying. Finally, the Mn-CDs powder dispersed in deionized water with a concentration of 0.25 mg mL^{-1} for further characterization and test.

2.3 Sample Preparation

Animal meat samples (chicken, carp, and duck meat) were obtained from a local fresh market in Zhengzhou City, China. The TC present in poultry meat samples was extracted using a McIlvaine buffer procedure according to previous reports [8,33]. The McIlvaine buffer solution was prepared by dissolving 11.8 g of CA, 13.72 g of Na_2HPO_4 , and 33.62 g of EDTA in 1 L of deionized water. Briefly, 5 g of a poultry meat sample was homogenized, placed in a glass

centrifuge tube, and the 2 mL of 20% TCA was added. The centrifuge tube was shaken well, 20 mL of McIlvaine buffer solution was added, and then the mixture was centrifuged for 15 min (5000 rpm). The obtained supernatant was filtered through a $0.45 \mu\text{m}$ PTFE filter, and the filtered solution was used for analysis.

2.4 Analytical Procedure for TC

First, 1.0 mL of the Mn-CDs solution (0.25 mg mL^{-1}) was added into a 10 mL graduated tube containing 5.0 mL of B-R buffer solution (pH 6.0). 1.0 mL of TC standard solution at different concentrations (or the sample solution) was placed to the above mixture. After diluting with deionized water to the required volume, the mixture was shaken thoroughly prior to the fluorescence measurements. Simultaneously, a reagent blank was also prepared without addition of either the TC standard solution or sample solution.

The FI of the emission peaks (360 nm) for the reagent blank (I_0) and the test solution (I) were obtained under an excitation wavelength of 300 nm. And $\log(I_0/I)$ was calculated for Spectrometric quantities.

3. RESULTS AND DISCUSSION

3.1 Characterization of Mn-CDs

The morphology of the obtained Mn-CDs was investigated by TEM. As shown in Fig. 1a, it could be observed that the Mn-CDs are spherically-shaped with a diameter of about $3.17 \pm 0.6 \text{ nm}$, and the lattice fringes of 0.21 nm was consistent with the (1 0 0) facet of graphite carbon [34]. FT-IR spectra in Fig. 1b were applied to characterize the functional groups on the surface of the Mn-CDs, which included pyridyl C-H, C=C and C=N. The peaks at 500 cm^{-1} may be attributed to a coordination band between the pyridyl N and Mn^{2+} .

XPS data was collected to investigate the status of elements in the Mn-CDs. The high resolution C1s (Fig. 1c) spectrum can be deconvoluted into four peaks and indicates the presence of C-N (287.7 eV), C-O/C=O (286.8 eV), C-C (285.5 eV) and C=C (284.6 eV) [35]. The peak at 641.0 eV in the high resolution Mn2p spectrum (Fig. 1d) reveals that Mn (II)-coordination is present in the Mn-CDs in the form of Mn-O.

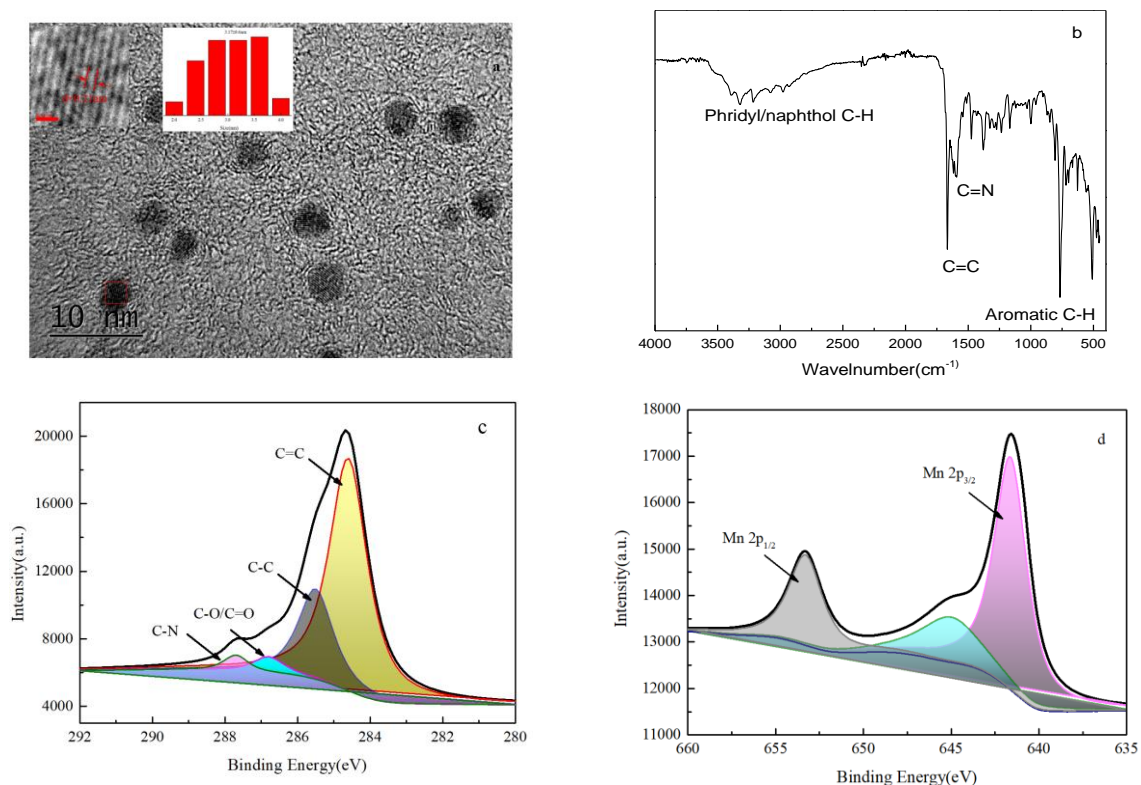


Fig. 1. (a) TEM image of the Mn-CDs. (b) FT-IR spectra of the Mn-CDs. (c) C1s and (d) Mn2p high resolution spectra of the Mn-CDs

Optical properties of the Mn-CDs were explored using ultraviolet-visible (UV-vis) and fluorescence spectroscopies. The Mn-CDs showed a characteristic absorption peak at 300 nm (Fig. 2a, line 1) and a red shift compared with the typical absorption peak of C=O group (prominent absorption band for the C=O group appeared at 289 nm), which was attributed to the coordination of Mn...O. The fluorescence excitation and emission spectra of the Mn-CDs was also showed in Fig. 2a (line 2 and line 3). When excited at 300 nm, the Mn-CDs showed the strongest emission intensity at approximately 360

nm. The fluorescence quantum yield (QY) of the Mn-CDs was calculated as 83% with quinine sulfate as the reference sample. The improvement in QY could be attributed to the Mn doping.

Furthermore, the effect of pH on the FI of the Mn-CDs was investigated, and the experimental results are shown in Fig. 2b. The FI of the Mn-CDs in basic media were much lower than those in acidic media, while the FI kept almost constant in the pH range of 1-3 and 7-10.

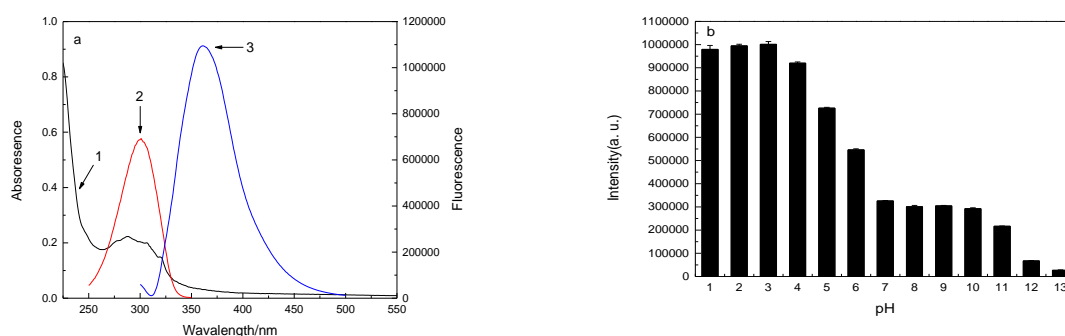


Fig. 2. (a) UV-vis absorption spectra (Curve 1) of the Mn-CDs, Excitation spectra (Curve2) and Emission spectra (Curve 3) of the Mn-CDs. (b) Effects of pH on FI of the Mn-CDs

3.2 Fluorescent Sensing of TC

The Mn-CDs were applied in fluorescent detection of TC with high selectivity and sensitivity. As shown in Fig. 3, the FI at 360 nm of the Mn-CDs could be effectively quenched with the increase of adding TC concentrations. Good linear response between $\log(I_0/I)$ and TC concentration is observed in the range of 0.1-200 μM with a 10 nM detection limit based on 3σ . The regression equation between $\log(I_0/I)$ and TC concentration (C , μM) was $\log(I_0/I) = 0.01614C + 0.01596$, and the relative standard deviation (RSD) was 2.1% ($c = 100 \mu\text{M}$). In addition, fluorescence quenching phenomenon was investigated using the Stern-Volmer equation: $I_0/I = K_{sv}C + 1$, where K_{sv} is the quenching constant (M^{-1}). The calculated value of K_{sv} was $4.50 \times 10^4 \text{ L mol}^{-1}$.

3.3 Selectivity for TC Detection

To verify the specificity of the Mn-CDs probe for TC, the influence of organic small molecules and metal ions were investigated. As shown in Fig. 4a, 100 μM TC and different organic compounds (AA, CA, Urea, Lys, Met, Arg, His, Phe, Tyr, α -Lac, Lac, Fru, Man, Sur, and Glu) were chosen to evaluate the selectivity of fluorescence response of the Mn-CDs. Compared to the control group, there was no significant difference in fluorescence quenching behavior of the Mn-CDs by TC in the presence of possible interfering compounds (100 μM), which indicates the high selectivity of the Mn-CDs probe for sensing TC.

Metal ions were also selected to investigate the selectivity of the Mn-CDs probe for TC (Fig. 4b). None of the metal ions (10 μM for Fe^{3+} ; 100 μM for other metal ions) had an obvious influence on FI of the Mn-CDs in the presence and absence of TC. Therefore, the fluorescent sensor demonstrated a high tolerance for the presence of metal ions, which is promising for detecting TC in water samples.

3.4 Fluorescence Quenching Mechanism

In order to elucidate the fluorescence quenching mechanism of the Mn-CDs by TC, fluorescence lifetime (FL) of the Mn-CDs and spectrum overlap between the Mn-CDs emission peak and absorption spectra of TC were studied. As can be seen from Fig. 5a, TC has strong characteristic absorption peak at 356 nm ($\epsilon = 1.5 \times 10^4 \text{ cm}^{-1} \text{ mol}^{-1} \text{ L}$), which shows large spectrum

overlap with the Mn-CDs emission peak (360 nm), therefore, the possible fluorescence quenching mechanism of the Mn-CDs by TC may be IFE or Förster resonance energy transfer (FRET). To verify the quenching mechanisms, FL measurements were carried out for the Mn-CDs in both the presence and absence of TC. The obtained results showed that the average FL of the Mn-CDs with (5.93 ns) and without (5.98 ns) TC did not change significantly, which indicated there is no FRET between the Mn-CDs and TC.

Therefore, the possible fluorescence quenching mechanism of the Mn-CDs by TC may be IFE. Recently, a simplified correction factor based on a mathematical model of IFE has been widely used to confirm IFE [36-38]. According to the mathematical model, the corrected FL of the Mn-CDs were calculated. It was found that the corrected FL of the Mn-CDs remained nearly unchanged as the TC concentrations increased. Therefore, it can be confirmed that the fluorescence quenching mechanism of the Mn-CDs by TC was IFE rather than static quenching. To further exclude the presence of static quenching, the absorption spectra of the TC, Mn-CDs and Mn-CDs-TC mixtures were recorded. It can be seen from Fig. 5b that there is no significant difference between the absorption spectra of Mn-CDs-TC mixtures and those of the sum value of the Mn-CDs and TC. This suggests that no Mn-CDs-TC complex was formed, and the presence of static quenching was excluded [37,39].

For an additional comparison, the analytical performance of the Mn-CDs probe and other CDs probes for TC reported previously are listed in Table 1. As the data shown in Table 1, the developed method based on the Mn-CDs has a comparable detection limit with a wider linear range. Additionally, the Mn-CDs were synthesized by a simple one-step hydrothermal procedure, and the sensing procedure based on IFE is simple and quick. Therefore, the Mn-CDs probe was selective and sensitive for TC detection with great convenience, low-cost and a short analytical time.

3.5 Determination of TC in Real Samples

To trace the feasibility of the sensor, the proposed method was applied to determine TC in different poultry meat samples using standard curve method. Analytical results are exhibited in Table 2, and the recoveries for the spiking

experiments were in the range of 102.1% to 115.1%. Based on the good stability and high selectivity of the Mn-CDs, the recovery

results indicate the excellent accuracy and reproducibility of the proposed method.

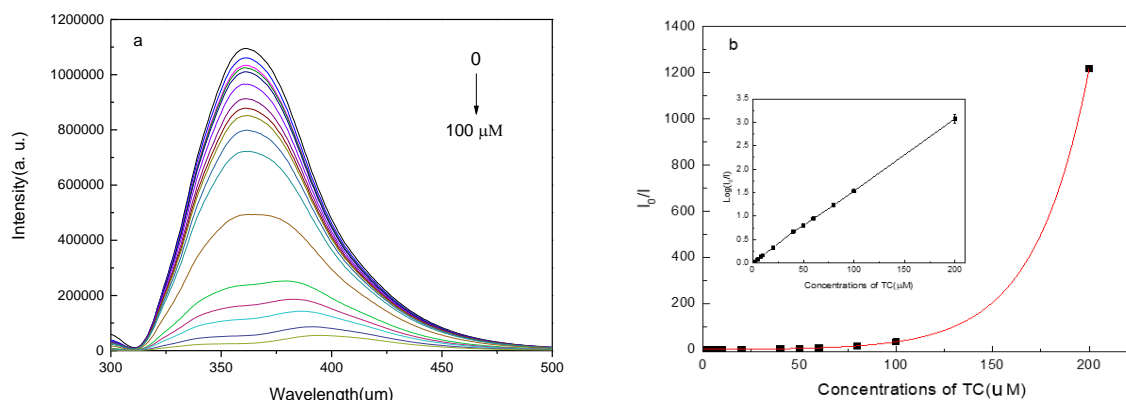


Fig. 3. Fluorescence quenching of the Mn-CDs by TC. (a) Fluorescence responses of the Mn-CDs in the presence of different concentrations of TC (0, 0.1, 0.2, 0.5, 0.8, 1, 2, 5, 8, 10, 20, 40, 50, 60, 80, 100 and 200 μM). (b) Dependence of I_0/I on the concentrations of TC. Inset: linear relationship between $\lg(I_0/I)$ and concentrations of TC

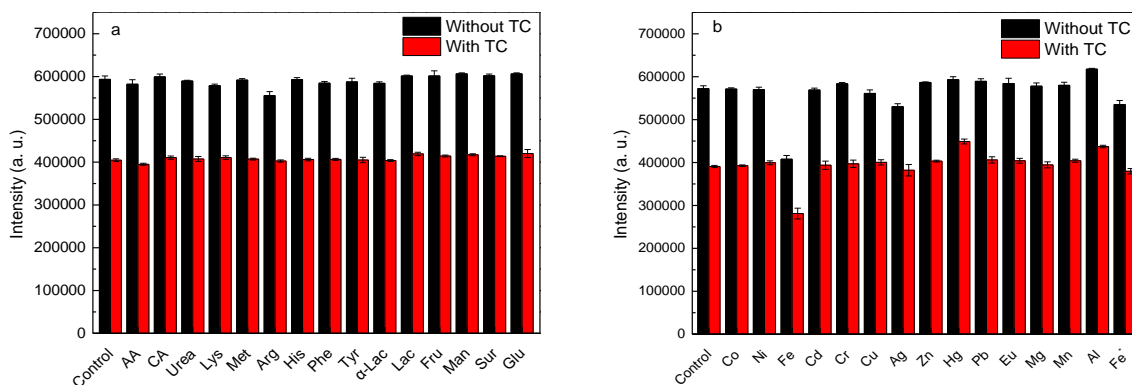


Fig. 4. Interferences of (a) other organic compounds and (b) metal ions in BR buffer (pH 3.0). Concentrations of TC, organic compounds, and metal ions are 100 μM (10 μM for substances indicated with *)

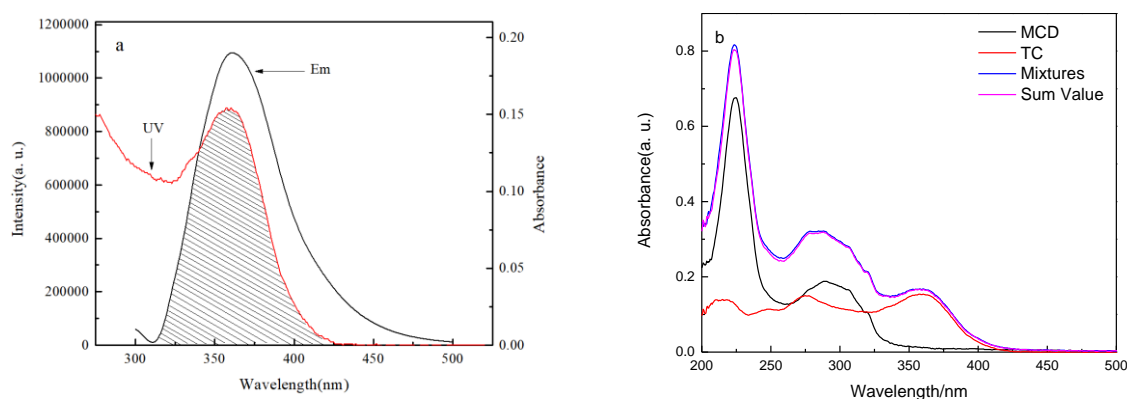


Fig. 5. Detection mechanism of TC. (a) UV-vis absorption spectra of TC and the fluorescence emission spectra of the Mn-CDs. (b) UV-vis absorption spectra of the Mn-CDs, TC, Mn-CDs-TC mixtures, and the sum value of absorbance of Mn-CDs and TC

Table 1. Comparative analytical performance from reported studies on fluorescent probes for TC

Probes	Mechanism	Detection limit	Linear range	References
Biomass derived CDs	Unspecified	230 nM	3.32-32.26 μ M	25
Xylan-derived CDs	IFE	6.49 nM	0.05-20 μ M	24
CDs coated with molecularly imprinted silica	IFE	9 nM	0.1-50 μ M	26
GQDs-Eu ³⁺ system	Unspecified	8.2 nM	0-20 μ M	21
Carbon nanoparticles	Unspecified	7.5 nM	0.06-8 μ M	27
Mn-CDs	IFE	10 nM	0.1-200 μ M	This work

Table 2. Determination of TC in poultry meat samples (n = 3, mean \pm SD, μ g g⁻¹)

Samples	Added value	Determined value	Recovery (%)
Chicken	0	-	-
	19.2	20.6 \pm 0.2	107.3%
	96.5	101.8 \pm 2.1	105.5%
Carp meat	0	-	-
	19.2	19.6 \pm 0.4	102.1%
	96.5	102.7 \pm 1.6	106.4%
Duck meat	0	-	-
	19.2	22.1 \pm 0.2	115.1%
	96.5	104.1 \pm 1.7	104.7%

4. CONCLUSION

In summary, we have successfully prepared Mn-CDs via a one-step hydrothermal procedure from PAN and MnCl₂, and the obtained Mn-CDs were used as fluorescent probe for selective and sensitive TC determination based on the mechanism of IFE. The developed method is a rapid analytical method which possesses high selectivity and sensitivity. The method has good practicability and has been successfully applied to the determination of TC in poultry meat samples.

ACKNOWLEDGEMENTS

This work was financially supported by the National Natural Science Foundation of China (Grant No. 21205028) and the open project (Grant No. GA2018007) of Engineering Technology Research Center for Grain & Oil Food, State Administration of Grain.

COMPETING INTERESTS

Authors have declared that no competing interests exist.

REFERENCES

1. Palominos RA, Mondaca MA, Giraldo A, Gustavo Peuela, Mansilla HD.

- Photocatalytic oxidation of the antibiotic tetracycline on TiO₂ and ZnO suspensions [J]. *Catal Today*. 2009;144:100-105.
2. Liu N, Xue-Xin GU, Neng-Sheng YE, Jing-Bo YU, Zhang Q, Huang HS, Hao XL. SPE-HPLC determination of tetracycline antibiotics residues in milk [J]. *Chin J Pharm Anal*. 2009;29:810-813.
3. Sun X, He X, Zhang Y, Chen L. Determination of tetracyclines in food samples by molecularly imprinted monolithic column coupling with high performance liquid chromatography [J]. *Talanta*. 2009;79:926-934.
4. Jing T, Wang Y, Dai Q, Xia H, Niu JW, Hao QL, Mei SR, Zhou YK. Preparation of mixed-templates molecularly imprinted polymers and investigation of the recognition ability for tetracycline antibiotics [J]. *Biosens Bioelectron*. 2010;25:2218-2224.
5. Ahmadi F, Shahbazi Y, Karami N. Determination of tetracyclines in meat using two phases freezing extraction method and HPLC-DAD [J]. *Food Anall Method*. 2014;8:1883-1891.
6. Commission Regulation No. 508/99. Official Journal of the European Communication 9, L60; 1999.
7. Yu H, Tao Y, Chen D, Wang Y, Yuan Z. Development of an HPLC-UV method for the simultaneous determination of

- tetracyclines in muscle and liver of porcine, chicken and bovine with accelerated solvent extraction [J]. *Food Chem.* 2011;124:1131-1138.
8. Shalaby AR, Salama NA, Abou-Raya SH, Emam WH, Mehaya FM. Validation of HPLC method for determination of tetracycline residues in chicken meat and liver [J]. *Food Chem.* 2011;124:1660-1666.
 9. Nebot C, Guarddon M, Seco F, Lglesias A, Miranda JM, Franco CM, Cepeda A. Monitoring the presence of residues of tetracyclines in baby food samples by HPLC-MS/MS [J]. *Food Control.* 2014;46:495-
 10. Zhou Q, Zhang Y, Wang N, Zhu L, Tang H. Analysis of tetracyclines in chicken tissues and dung using LC-MS coupled with ultrasound-assisted enzymatic hydrolysis [J]. *Food Control.* 2014;46:324-331.
 11. Kowalski P. Capillary electrophoretic method for the simultaneous determination of tetracycline residues in fish samples [J]. *J Pharmaceut and Biomed.* 2008;47:487-493.
 12. Anastasopoulos P, Timotheou-Potamia M. Chemiluminescence determination of tetracyclines via aluminum sensitized fluorescence [J]. *Anal Lett.* 2011;44:25-37.
 13. Shen L, Chen J, Li N, He P, Li Z. Rapid colorimetric sensing of tetracycline antibiotics with in situ growth of gold nanoparticles [J]. *Anal Chim Acta.* 2014;839:83-90.
 14. Kwon YS, Ahmad Raston NH, Gu MB. An ultra-sensitive colorimetric detection of tetracyclines using the shortest aptamer with highly enhanced affinity [J]. *Chem Commun (Camb).* 2014;50:40-42.
 15. Hosseini M, Mehrabi F, Ganjali MR, Norouzi P. A fluorescent aptasensor for sensitive analysis oxytetracycline based on silver nanoclusters [J]. *Luminescence.* 2016;31:1339-1343.
 16. Xu N, Yuan Y, Yin J-H, Wang X, Meng L. One-pot hydrothermal synthesis of luminescent silicon-based nanoparticles for highly specific detection of oxytetracycline via ratiometric fluorescent strategy [J]. *RSC Adv.* 2017;7:48429-48436.
 17. Leng F, Zhao XJ, Wang J, Li YF. Visual detection of tetracycline antibiotics with the turned on fluorescence induced by a metal-organic coordination polymer [J]. *Talanta.* 2013;107:396-401.
 18. Tan HL, Ma CJ, Song YH, Xu FG, Chen SH, Wang L. Determination of tetracycline in milk by using nucleotide/lanthanide coordination polymer-based ternary complex [J]. *Biosens Bioelectron.* 2013;50:447-452.
 19. Tan H, Chen Y. Silver nanoparticle enhanced fluorescence of europium (iii) for detection of tetracycline in milk [J]. *Sensor Actuat B: Chem.* 2012;173:262-267.
 20. Yang X, et al. Novel and remarkable enhanced-fluorescence system based on gold nanoclusters for detection of tetracycline [J]. *Talanta.* 2014;122: 36-42.
 21. Li W, Zhu J, Xie G, Ren Y, Zheng Y-Q. Ratiometric system based on graphene quantum dots and Eu³⁺ for selective detection of tetracyclines [J]. *Anal Chim Acta.* 2018;1022:131-137.
 22. Gao C, Liu Z, Chen J, Yan Z. A novel fluorescent assay for oxytetracycline hydrochloride based on fluorescence quenching of water-soluble CdTe nanocrystals [J]. *Luminescence.* 2013;28:378-383.
 23. Elmizadeh H, Soleimani M, Faridbod F, Bardajee GR. Fabrication and optimization of a sensitive tetracycline fluorescent nano-sensor based on oxidized starch polysaccharide biopolymer-capped CdTe/ZnS quantum dots: Box-behnken design [J]. *J Photoch Photobio A.* 2018;367:188-199.
 24. Yang P, Zhu Z, Chen M, Chen W, Zhou X. Microwave-assisted synthesis of xylan-derived carbon quantum dots for tetracycline sensing [J]. *Opt Mater.* 2018;85:329-336.
 25. Qi HJ, Teng M, Liu M, Liu SX, Liu J, Yu HP, Teng CB, Huang ZH, Guo ZH. Biomass-derived nitrogen-doped carbon quantum dots: Highly selective fluorescent probe for detecting Fe⁽³⁺⁾ ions and tetracyclines [J]. *J Colloid Interface Sci.* 2019;539:332-341.
 26. Yang J, Lin ZZ, Nur A-Z, Lu Y, Wu MH, Zeng J, Chen XM, Huang ZY. Detection of trace tetracycline in fish via synchronous fluorescence quenching with carbon quantum dots coated with molecularly imprinted silica [J]. *Spectrochim Acta A.* 2018;190:450-456.
 27. Yang X, Luo Y, Zhu S, Feng Y, Zhuo Y, Dou Y. One-pot synthesis of high fluorescent carbon nanoparticles and their applications as probes for detection of tetracyclines [J]. *Biosens Bioelectron.* 2014;56:6-11.

28. Zu F, Yan F, Bai Z, Xu J, Wang Y, Huang Y, Zhou X. The quenching of the fluorescence of carbon dots: A review on mechanisms and applications [J]. *Microchim Acta*. 2017;184:1899-1914.
29. Ye SL, Huang JJ, Luo L, Fu HJ, Sun YM, Shen YD, Lei HT, Xu ZL. Preparation of carbon dots and their application in food analysis as signal probe [J]. *Chinese J Anal Chem*. 2017;45:1571-1581.
30. Gao X, Du C, Zhuang Z, Chen W. Carbon quantum dot-based nanoprobe for metal ion detection [J]. *J Mater Chem C*. 2016;4:6927-6945.
31. Zhou J, Zhou H, Tang JB, Deng S, Yana F, Li WJ, Qu MH. Carbon dots doped with heteroatoms for fluorescent bioimaging: A review [J]. *Microchim Acta*. 2016;184:343-368.
32. Wang Y, Zhang Y, Jia MY, Meng H, Li H, Guan YF, Feng L. Functionalization of carbonaceous nanodots from Mn(II) - coordinating functional knots [J]. *Chem*. 2015;21:14843-14850.
33. Cinquina AL, Longo F, Anastasi G, Giannetti L, Cozzani R. Validation of a high-performance liquid chromatography method for the determination of oxytetracycline, tetracycline, chlortetracycline and doxycycline in bovine milk and muscle [J]. *J Chromatogr A*. 2003;987:227-233.
34. Wang Z, Yuan F, Li X, Zhong H, Fan L, Yang S. 53% efficient red emissive carbon quantum dots for high color rendering and stable warm white-Light-Emitting diodes [J]. *Adv Mater*. 2017;29:1702910.
35. Kaur M, Mehta SK, Kansal SK. A fluorescent probe based on nitrogen doped graphene quantum dots for turn off sensing of explosive and detrimental water pollutant, TNP in aqueous medium [J]. *Spectrochim Acta A*. 2017;180:37-43.
36. Gu Q, Kenny JE. Improvement of inner filter effect correction based on determination of effective geometric parameters using a conventional fluorimeter [J]. *Anal Chem*. 2009;81:420-426.
37. Liu H, Xu C, Bai Y, Liu L, Liao D, Liang J, Liu L, Han H. Interaction between fluorescein isothiocyanate and carbon dots: Inner filter effect and fluorescence resonance energy transfer [J]. *Spectrochim Acta A*. 2017;171:311-316.
38. Nettles CB, Hu J, Zhang D. Using water raman intensities to determine the effective excitation and emission path lengths of fluorophotometers for correcting fluorescence inner filter effect [J]. *Anal Chem*. 2015;87:4917-4924.
39. Fan HH, Xiang GQ, Wang YL, Zhang H, Ning KK, Duan JY, He LJ, Jiang XM, Zhao WJ. Manganese-doped carbon quantum dots-based fluorescent probe for selective and sensitive sensing of 2,4,6-trinitrophenol via an inner filtering effect [J]. *Spectrochim Acta A*. 2018;205:221-226.

© 2021 Su et al.; This is an Open Access article distributed under the terms of the Creative Commons Attribution License (<http://creativecommons.org/licenses/by/4.0>), which permits unrestricted use, distribution, and reproduction in any medium, provided the original work is properly cited.

Peer-review history:

The peer review history for this paper can be accessed here:
<https://www.sdiarticle4.com/review-history/70742>